Local Order, Energy, and Mobility of Water Molecules in the Hydration Shell of Small Peptides

Manish Agarwal,[†] Hemant R. Kushwaha,[‡] and Charusita Chakravarty*,[†]

Department of Chemistry, Indian Institute of Technology-Delhi, New Delhi 110016, India, and School of Information Technology, Jawaharlal Nehru University, New Delhi 110067, India

Received: September 21, 2009

The extent to which the presence of a biomolecular solute modifies the local energetics of water molecules, as measured by the tagged molecule potential energy (TPE), is examined using molecular dynamics simulations of the β-hairpin of 2GB1 and the α-helix of deca-alanine in water. The CHARMM22 force field, in conjunction with the TIP3P solvent water model, is used for the peptides, with simulations of TIP3P and SPC/E water used as benchmarks for the behavior of bulk solvent. TIP3P water is shown to have significantly lower local tetrahedral order and higher binding energy than SPC/E at the same state point. The TIP3P and SPC/E water models show very similar dynamical correlations in the TPE fluctuations on frequency scales greater than 0.1 cm^{-1}. In addition, the two models show the same linear correlation between mean tetrahedral order and binding energy, suggesting that the relationship between choice of water models and simulated hydration behavior may involve a complex interplay of static and dynamic factors. The introduction of a peptide in water modifies the local TPE of water molecules as a function of distance from the biomolecular interface. There is an oscillatory variation in the TPE with distance from the peptide for water molecules lying outside a 3 Å radius and extending to at least 10 Å. These variations are of the order of 2−5% of the bulk TPE value and are anticorrelated with variations in local tetrahedral order in terms of locations of maxima and minima, which may be understood in terms of the relative contribution of van der Waals and Coulombic contributions to the TPE. The distance-dependent variations in local order and energetics are essentially the same for the β-hairpin of 2GB1 as well as deca-alanine. Within a radius of 3 Å, the perturbation of the solvent structure is very significant with local TPEs that are 10−15% lower than the bulk value. The chemical identity of side-chain residues and the secondary structure play an important role in determining residue-dependent variations in the TPEs. The variation in the residue-dependent tagged molecule potential energies is of the order of 3−5%, while the local residence times vary by a factor of approximately 5. The correlation of the local residence times with the local energetics within the innermost hydration layer is weak, though charged residues typically have low binding energies and large residence times.

1. Introduction

The organization of water at biomolecular interfaces is crucial for understanding the role of water as a solvent in biological processes.[1−5] Bulk water has several unusual features which play an essential role in hydration. The relatively large dipole moment and polarizability of water result in a very high dielectric constant and make water an excellent solvent for ionic or polar solutes, including polyelectrolytes such as DNA. Each water molecule can form four hydrogen bonds with a bond energy between 5 and 10 k_BT at room temperature. As a consequence, liquid water has a fluctuating, three-dimensional network structure with local tetrahedral order that has been associated with the presence of anomalous thermodynamic and kinetic behavior.[6−8] The reorganization of the hydrogen-bonded network around nonpolar solutes underlies the hydrophobic interactions responsible for the three-dimensional folded structures of proteins in aqueous media.[9] Neutron scattering studies show that water typically forms a layer about 3 Å in width around a protein or peptide surface which has significantly higher density, by as much as 25%, compared to bulk water.[10] Structural changes in terms of the disruption of the hydrogen-bonded network of water are largely localized within this layer. Dynamical changes involving disruption of cooperative reorganizations of the solvent are much more significant and potentially longer-ranged. Water dynamics, as measured by rotational correlation times and local diffusivities, appears to slow down by factors of 4−7 around a globular protein. Water dynamics at 298 K seems to be characterized by at least two distinct time scales: an ultrafast (sub-100-fs) time scale and a slower one between 20 and 40 ps.[2] The structure and dynamics of the hydration layer of water thus reflect a complex interplay between entropic, energetic, and steric factors.

There have been significant recent advances in our understanding of the relationship between the liquid state anomalies and phase diagram of water, especially with regard to the relationship between structural order, thermodynamic properties, and mobility in the liquid state.[6−8,11−14] The implications of our improved understanding of water for understanding aqueous solvation are beginning to emerge, though most of the studies are restricted to relatively simple solutes.[9,10,15−17] In this work, we explore whether measures of local order and energetics that have been found to be useful for bulk water are useful for characterizing structure and dynamics in the hydration layer of small peptides.

* Corresponding author. Phone: (+)91-11-2659-1510. Fax: (+)91-11-2686-2122. E-mail: charus@chemistry.iitd.ernet.in.
[†] Indian Institute of Technology-Delhi.
[‡] Jawaharlal Nehru University.

10.1021/jp909090u
Published on Web 10/28/2009

Local tetrahedral order is one of the distinctive features of the hydrogen-bonded network of water.[7] The loss of this local orientational order with compression or heating can be connected with the anomalous properties of bulk water, such as a rise in diffusivity on isothermal compression.[7,11,12] Evidence from neutron diffraction suggests that different solutes alter the degree of local tetrahedrality to different extents, with those that enhance the tetrahedrality being ones that dissolve or mix readily with water.[18] To our knowledge, tetrahedral order in the hydration layer of biomolecular solutes has been examined to only a limited extent; for example, in the case of small sugar molecules and a small protein.[19,20]

In recent studies on water, methanol, as well as liquids with water-like anomalies, we have found it useful to focus on the tagged molecule potential energy (TPE), u, which corresponds to the interaction energy of an individual water molecule with all other molecules in the system.[21−25] This is equivalent to the binding energy of an individual water molecule at a particular location at a given instant of time. Temporal correlations in the TPE are sensitive to local librational modes as well as network reorganizations involving two or more molecules. As a consequence of this multiple time-scale behavior of the dynamics of water and other network forming liquids, the power spectra of the fluctuations in the TPE show a region of multiple time scale (MTS) or $1/f^{\alpha}$ behavior. In the case of water and methanol, the exponent α of the MTS regime is found to be correlated with the diffusivity over a fairly wide range of temperatures and densities. The mean tagged potential energy in bulk water can be demonstrated to be the leading contribution to the chemical potential by performing a cumulant expansion of the Widom particle insertion expression for the chemical potential.[26−28] To our knowledge, the tagged potential or binding energy of water molecules in the hydration layer of peptides or proteins has received only limited attention,[29] though the interaction energy of protein residues with water has been extensively studied.[30−33]

As representative examples of peptides, we consider the 16-residue C-terminal fragment of 2GB1 and deca-alanine. The former has a stable β-hairpin structure in aqueous solution under standard conditions and has been therefore studied extensively, both experimentally and theoretically.[34−41] Polyalanine fragments of various sizes are known to form α-helices in solution. The deca-alanine oligomer has been extensively used as a model for understanding helix−coil transitions and the associated free energy landscapes.[42−45] We use the TIP3P potential to model the aqueous environment of the peptide, since the CHARMM22 force field is parametrized with this water model.[46,47] The TIP3P water model is known, however, to be poorer than other three-site effective pair potentials for water, such as SPC/E, in terms of reproducing the bulk properties of water, such as the liquid state anomalies and the phase diagram.[12,48,49] We therefore compare the behavior of the tagged molecule potential energies and the tetrahedral order parameter of the bulk TIP3P and SPC/E water to assess the possible effects of using different solvent models to understand the hydration layer structure and dynamics.

To summarize, the purpose of this study is to examine the usefulness of the tagged molecule potential energy, known to be a good measure of local order and energetics in bulk water, as a convenient quantity for characterizing the static and dynamic behavior of water molecules in the neighborhood of small peptides. The tagged potential energies of water molecules in the vicinity of the 2GB1 β-hairpin and deca-alanine α-helical peptides were computed using the CHARMM22 force field in conjunction with the TIP3P water model. The bulk properties of TIP3P and SPC/E water are first discussed to provide a benchmark for understanding the effect of the biomolecular interfaces on water structure and the possible consequences of using different water models when studying hydration. The tagged potential energy and tetrahedral order are studied as a function of distance from the biomolecular interface and show a strong negative correlation, similar to that of bulk water, except very close to the peptide surface at very low temperatures. The residue-dependent variations in the tagged potential energy of water molecules within the hydration layer are also studied, and the correlation of these static measures of local order and energetics with the local residence times of water molecules in the neighborhood of different amino acid residues is examined.

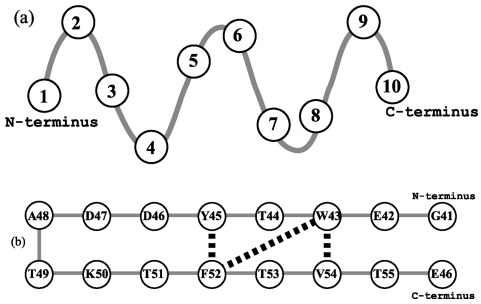

Figure 1. Schematic diagrams of (a) the α-helix of deca-alanine and (b) the β-hairpin of 2GB1. The dashed lines connect residues interacting with via hydrophobic side chains.[34]

2. Computational Details

2.1. Systems. Bulk water was modeled using cubic simulation cells of 256 water molecules using both the TIP3P and SPC/E water models.[50,51]

We initiate the molecular dynamics simulations with the folded conformation of the two peptides. To generate the initial configuration for the β-hairpin fragment 2GB1, the 16-residue-long C-terminal (GEWTYDDATKTFTVTE) fragment of the immunoglobin binding domain of streptococcal protein G (PDB ID: 2GB1) was extracted and solvated using 1741 TIP3P water molecules. The pH conditions were assumed to be such that the C-terminal and the N-terminal did not carry charges while the two aspartic acid and two glutamic acid residues were assigned negative charges and the lysine side chain was assigned a positive charge. Hence, three of the waters were replaced by sodium ions to balance the net −3 charge of the peptide. The Tcl/Tk interface of the Visual Molecular Dynamics (VMD) package was used as a tool to prepare the initial input configurations of the peptide in TIP3P solvent.[52] The solvation and ionization were done using the "solvate" and "autoionize" plugins of VMD, respectively. The resulting cubical box was used for further simulations. The initial configuration of the α-helix of the oligo-peptide deca-alanine was taken from ref 44 and similarly solvated using the VMD plugins described above. The resulting system consisted of 1910 TIP3P water molecules surrounding the helix in a cubical box.

The CHARMM22 force field with TIP3P water as solvent was used for the simulations of solvated peptides. Schematic diagrams of the β-hairpin structure of 2GB1 and the α-helix of deca-alanine are shown in Figure 1.

2.2. Molecular Dynamics. Molecular dynamics simulations of 256 SPC/E and TIP3P water molecules were performed using the DL_POLY software package.[53] The equations of motion were integrated using the Verlet leapfrog algorithm with rigid-body constraints implemented with the SHAKE algorithm. A time step of 1 fs was used, and production run lengths were 4 ns. Simulations were carried out for temperatures ranging from

170 to 300 K and 220 to 300 K for TIP3P and SPC/E, respectively, in the canonical ensemble (NVT) with densities ranging from 0.90 to 1.30 g cm^{-3}. Tagged potential energy data was written to disk for a subset of 64 molecules every 5 steps for the 300 K and 1.0 g cm^{-3} state point.

Simulations of the solvated β-hairpin of 2GB1 and the α-helix of deca-alanine were carried out using the NAMD software package.[54] Cubic simulation cells of the solvated peptides, prepared in their folded configurations as described in section 2.1, were subjected to conjugate gradient energy minimization so as to eliminate any stresses and steric conflicts arising during system preparation. The energy minimized system was then subjected to a heating of 1 K per 2500 steps to reach 200, 300, and 400 K. The heating was carried out in the isobaric−isothermal (NPT) ensemble at 1 atm pressure. At each of these three temperatures, the systems were further equilibrated in the NPT ensemble until the volume and temperature attained equilibrium values. The resulting configurations were used for collecting statistics in the microcannonical ensemble (NVE) using a 2 fs time step over 10^6 steps, corresponding to 2 ns production runs. The resulting boxes were of 36.9, 37.6, and 38.96 Å for the β-hairpin of 2GB1 and 37.8, 38.5, and 40.1 Å for the α-helix of deca-alanine, respectively, for 200, 300, and 400 K.

Particle mesh Ewald was used to account for long-range electrostatic contributions to configurational energy. Rigid bonds were handled using the RATTLE algorithm. Short-range interactions were computed using a potential cutoff corresponding to half the total box length. Configurations were stored every 100 steps (0.2 ps).

2.3. Observables. ***Local Structural Order.*** Local ordering of water molecules can be effectively quantified by the tetrahedral order parameter q_{tet}:

$$q_{tet} = 1 - \frac{3}{8}\sum_{j=1}^{3}\sum_{k=j+1}^{4}(\cos\psi_{jk} + 1/3)^2 \qquad (1)$$

where ψ_{jk} is the angle between the bond vectors $\mathbf{r}_{ij}$ and $\mathbf{r}_{ik}$, where j and k label the four nearest neighbor atoms of the same type.[7,55] For water molecules in the vicinity of the peptide, we extend this definition to include heavy atoms of the peptide (C, N, O, etc.) in the definition of the neighbors of the oxygen atom of a selected water molecule.

Binding Energy and Tagged Potential Energy. The binding energy associated with a single water molecule ΔU_{bind} is given by[29]

$$\Delta U_{bind} = U_{tot} - U_{N-1} \qquad (2)$$

where U_{tot} is the total configurational energy of the N-atom system and U_{N-1} is the configurational energy when a specific water molecule is artificially isolated or removed from the configuration, keeping the positions and interactions of all other atoms unchanged. This definition of binding energy is identical to the tagged potential energy (TPE) of the molecule, u, where the sum is over interactions of the tagged species with all others.[11,21,22,24] When the interactions in the system are pair-additive, then one can write that $U = (0.5/N)\sum_i u_i$, where the index i runs over all atoms in the system. The molecular tagged potential energy requires a summation over all constituent atoms of a molecule. In previous work, we have discussed the decomposition of u into

$$u = u_{coul} + u_{vdW} \qquad (3)$$

where u_{coul} and u_{vdW} are the contributions from Coulombic and van der Waals interactions. The Coulombic contribution can be written as the sum of contributions from real space, reciprocal space, and self-correction terms:

$$u_{coul} = u_{rec} + u_{real} + u_{self} \qquad (4)$$

In the case of the bulk water simulations using the DL_POLY code, we have directly evaluated the tagged particle energy within the forces subroutine, while, in the case of NAMD simulations, we have used a built-in option to evaluate the pair interaction between two selected groups of atoms.[56]

Residence Times. As a measure of molecular mobility, we use the local residence times (τ) of water molecules defined in terms of the survival probability function, $F_S(t)$, which represents the probability that a water molecule remains within a particular region continuously for a period of time t. Assuming that the time between successive stored configurations is sufficiently small that significant displacement of water molecules is unlikely, one can define

$$F_S(t) = \sum_{j=1}^{N_W}\frac{1}{t_{run} - t + 1}\sum_{t_0}^{t_{run}-t_0} f_j(\mathbf{r}, t_0, t_0 + t) \qquad (5)$$

where $f_j(\mathbf{r}, t_0, t_0 + t)$ is unity when the water molecule j is present at location $\mathbf{r}$ continuously from time t_0 to $t_0 + t$, and otherwise zero. N_W is the total number of water molecules; t_{run} is the length of the simulation. The location $\mathbf{r}$ has been defined to be either the entire hydration shell or a subregion of the hydration shell in the neighborhood of a specific peptide residue. The exact choice of hydration shell radius is discussed in section 3.2. The survival probability function $F_S(t)$ typically shows a sharp initial decay followed by an intermediate region which can be fitted by an expression of the form $\ln(F_S(t)) = -t/\tau + c$ to yield the survival time τ_S. Figure 2 shows the $F_S(t)$ function at 200 and 300 K for residue 41 of the β-hairpin of 2GB1. Following ref 10, we ignore the initial fast decay and fit the central portion of the survival probability function to an exponential form to extract the residence time, τ.

An alternative definition of local residence times has been used in several studies, for bulk water as well as water near interfaces,[29,57−59] which do not appear to explicitly impose a continuous presence at a given location over the length of time t.

3. Results and Discussion

3.1. Comparison of Bulk TIP3P and SPC/E Water. In this section, we consider the behavior of tagged molecule potential energies in bulk TIP3P and SPC/E water in order to compute the corresponding static distributions, the relationship between local order and energetics, and the dynamical correlations in the fluctuations of the local energies.

Figure 3 shows the tetrahedral order parameter distribution, $P(q_{tet})$, for TIP3P water at 200 and 300 K at 1 g cm^{-3}. Also shown is $P(q_{tet})$ for SPC/E water at 300 K and 1.0 g cm^{-3}. The bimodal order parameter distribution of SPC/E water at 300 K is characteristic of the region of anomalous liquid state behavior of water, where isothermal compression results in increasing local tetrahedral order.[7,11] In the case of TIP3P water, the $P(q_{tet})$

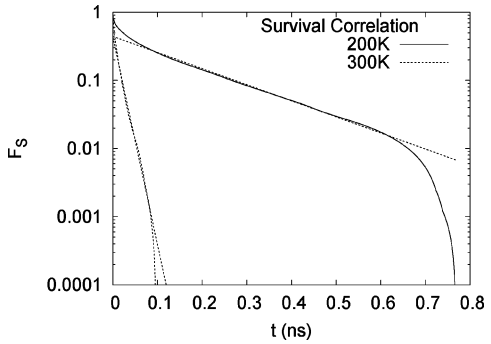

Figure 2. Time correlation functions for the β-hairpin of 2GB1 at 200 and 300 K for the survival correlation function. The lines denote the fitting of the linear portion of the curves. The correlation times are 184 and 14.26 ps, respectively.

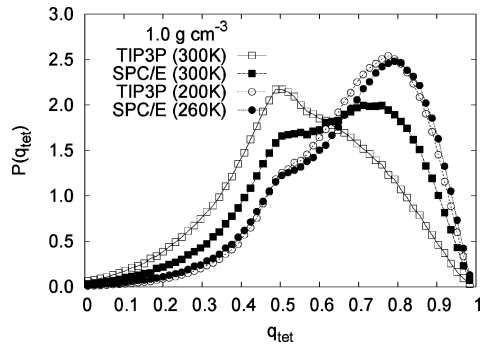

Figure 3. Normalized distribution of tetrahedral order parameter q_{tet} for bulk TIP3P and SPC/E at 1.0 g cm^{-3}.

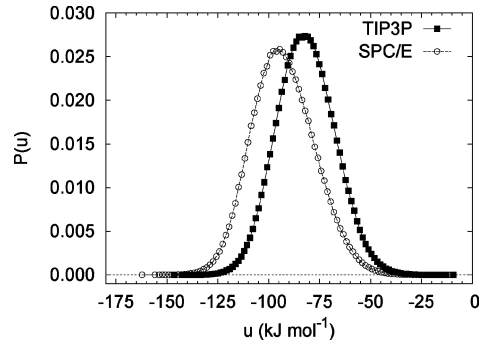

Figure 4. Static tagged potential energy distributions for SPC/E and TIP3P under ambient conditions (1.00 g cm^{-3}, 300 K).

distribution shows no evidence for q_{tet} values above 0.75, indicating that a tetrahedrally structured local environment for the water molecules is relatively rare in the TIP3P model under ambient conditions. At 200 K, however, TIP3P water does show significant local tetrahedral order and closely mimics the $P(q_{tet})$ distribution of SPC/E water at 260 K. This is consistent with other recent studies indicating that the liquid state anomalies of TIP3P water occur below ≈200 K which is much lower than that of SPC/E water (≈260 K) as well as real water (≈280 K).[12,49,60−62]

Figure 4 compares the tagged particle potential energy distributions, $P(u)$, of TIP3P and SPC/E water at 300 K at 1 g cm^{-3}. At this temperature, both distributions are Gaussian-like with the $\langle u \rangle$ being −92.61 and −82.14 kJ mol^{-1} for SPC/E and TIP3P water, respectively. Despite the apparent difference in the shapes of the $P(q_{tet})$ and $P(u)$ distributions, Figure 5 shows that the ensemble-averaged values, $\langle q_{tet} \rangle$ and $\langle u \rangle$, show a strong negative linear correlation along individual isochores. This correlation between high tetrahedral order and low tagged

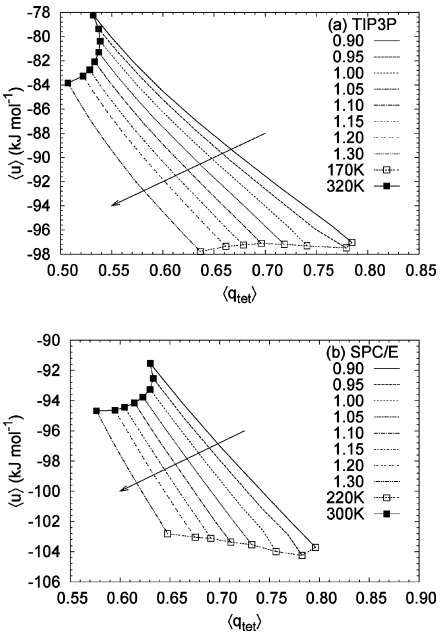

Figure 5. Correlation plot of tetrahedral order q_{tet} and average tagged potential energy $\langle u \rangle$ for (a) TIP3P and (b) SPC/E for densities in the range 0.90−1.30 g cm^{-3} and temperatures in the ranges 170−320 K (TIP3P) and 220−300 K (SPC/E). The arrows show the direction of increasing density. State points lying on isochores are connected with lines. The lowest and highest isotherms are also connected.

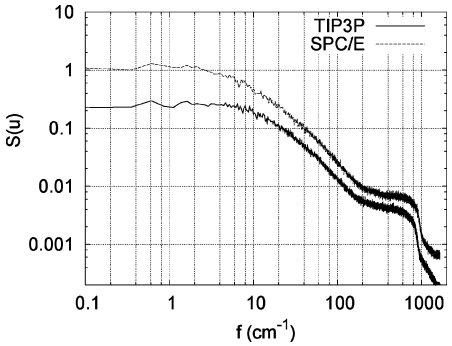

Figure 6. Power spectrum of bulk SPC/E and TIP3P water models under ambient conditions (1.00 g cm^{-3}, 300 K). Note that the amplitude of the SPC/E spectrum has been shifted by a multiplicative factor of 2 for ease of comparison.

potential energy has been previously suggested for TIP5P water.[60] Note that the $\langle q_{tet} \rangle$ versus $\langle u \rangle$ behavior along isotherms is nonmonotonic.

Figure 6 shows the power spectrum associated with fluctuations in the tagged particle potential energy of SPC/E and TIP3P water at 300 K. The power spectrum of the time-dependent TPE, $u(t)$, is defined as

$$S_u(f) = \lim_{T\to\infty} \frac{1}{T} \left| \int_{-T/2}^{T/2} u(t) e^{2\pi i f t} \, dt \right|^2 \qquad (6)$$

In an earlier set of studies, we have shown that the tagged potential energy of water is sensitive to the dynamical fluctuations of the network, including relatively high-frequency librations, O−O stretches, O−O−O bends, and higher-level network vibrations. As a consequence of a multiplicity of time scales, water as well as other network forming liquids show a $1/f^{\alpha}$ behavior in the $S_u(f)$ spectra.[21−25,63] Figure 6 shows that the key features of the $S_u(f)$ spectra of TIP3P and SPC/E water are

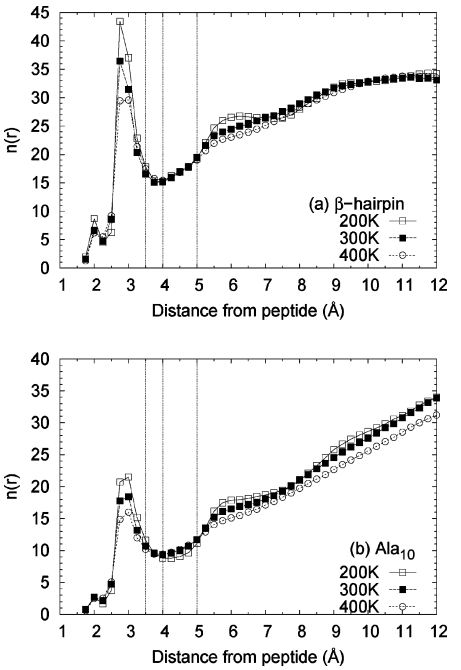

Figure 7. Number of molecules $n(r)$ as a function of distance from the protein surface at 200, 300, and 400 K for (a) the β-hairpin of 2GB1 and (b) the α-helix of deca-alanine. The vertical lines indicate, respectively, from left to right 3.5, 4.0, and 5.0 Å from the peptide surface. The total number of water molecules within these are, respectively, 142, 173, and 243 for the β-hairpin of 2GB1 and 78, 96, and 135 for the α-helix of deca-alanine.

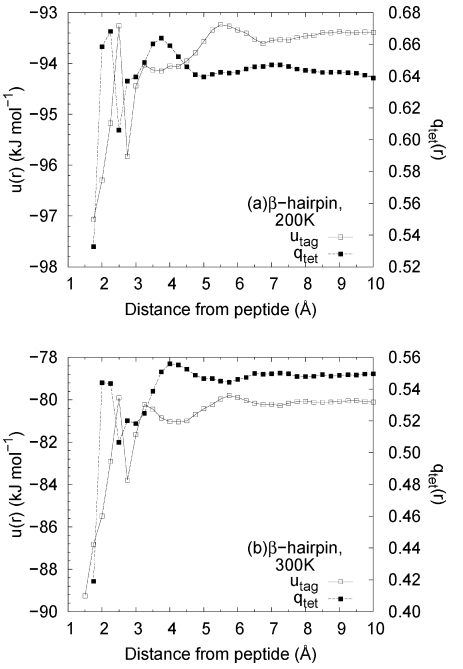

Figure 8. Variation of q_{tet} and u with distance from the protein for the β-hairpin of 2GB1 at (a) 200 K and (b) 300 K. $\langle u \rangle$ at 300 K and 1.00 g cm^{-3} is −82.11 kJ mol^{-1}, and that at 399 K and 1.30 g cm^{-3} is −85.29 kJ mol^{-1}.

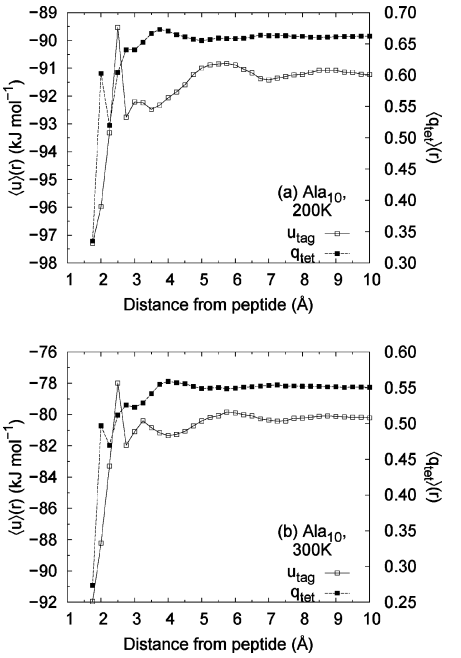

Figure 9. Variation of q_{tet} and u with distance from the protein for the α-helix of deca-alanine at (a) 200 K and (b) 300 K.

virtually identical at 300 K and 1 g cm^{-3}: (i) a broad librational peak between 300 and 800 cm^{-1}; (ii) a $1/f^{\alpha}$ region between 10 and 200 cm^{-1}; (iii) a crossover to white noise behavior around 4 cm^{-1}.[64] It is interesting to note that the strong similarity in the spectrum of intrinsic dynamical time scales in the two water models, despite the significant differences in static order and energetics. It suggests that the TIP3P model may be comparable to SPC/E when studying hydration dynamics on short time scales, though equilibrium dynamical properties such as diffusivities are known to be different.[62]

3.2. Water Structure and Energetics as a Function of Distance from the Biomolecular Interface. In this section, we consider the ordering of TIP3P water around the β-hairpin of 2GB1 and the α-helix of deca-alanine. We first consider the number of water molecules, $n(r)$, as a function of distance from the biomolecular surface. This is evaluated in the simulations by monitoring the number of water molecules with O atoms at a distance between r and $r + \Delta r$ from any one of the α-carbons of the peptide backbone with $\Delta r = 0.25$ Å. Figure 7 shows the behavior of $n(r)$ at 200, 300, and 400 K for both peptides. The effect of temperature is seen largely on the sharp peak associated with the sharp nearest neighbor shell and to a lesser extent on the broad shoulder associated with the second neighbor shell. The broad minimum between 3 and 5 Å separates the relatively dense hydration layer from the second neighbor shell and is essentially unchanged by variations in temperature. We found no significant differences in static properties of the hydration shell if cutoff distances ranging from 3.5 to 5.0 Å were used in defining the hydration layer. We have therefore defined the hydration layer as all water molecules with O atoms lying within 5 Å of at least one of the α-carbon atoms of the peptide backbone. Within the hydration layer, all water molecules lying within 5 Å of the α-carbon of a given amino acid residue were assigned to the corresponding residue when computing residue-dependent variations in local properties. This definition does imply that a few of the water molecules may be in the neighborhood of more than one residue.

The distance-dependent tetrahedral order, $q_{tet}(r)$, and tagged molecule potential energy, $u(r)$, functions were computed by averaging over the entire run the corresponding observables for all water molecules with their oxygen atoms lying within a distance r and $r + \Delta r$, where $\Delta r = 0.25$ Å. Figures 8 and 9 show $q_{tet}(r)$ and $u(r)$ for the β-hairpin as well as deca-alanine at 200 and 300 K.

We first consider the β-hairpin structure at 300 K. In the limit of large r, both $q_{tet}(r)$ and $u(r)$ reach an asymptotic value close

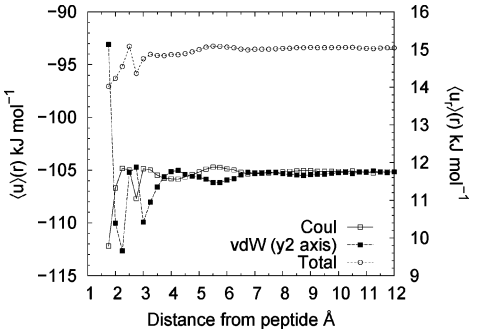

Figure 10. Variation of the components of tagged potential energy, i.e., Coulombic and vdW, for the β-hairpin of 2GB1 at 300 K with distance from the peptide.

to that of bulk water. For r values between 2.5 and 10 Å, $q_{tet}(r)$ and $u(r)$ are anticorrelated, with maxima in one quantity being mirrored by minima in the other quantity. Strong anticorrelation between the two quantities can also be observed at 200 K for r greater than 3 Å. For r values less than 3 Å, i.e., well within the first hydration layer, however, the correlation between local tetrahedral order and TPE breaks down. The maximum and minimum values of $\langle u \rangle$ observed in bulk TIP3P water at 300 K are -85.33 at 1.3 g cm^{-3} and -78.975 at 0.85 g cm^{-3}; the range of variation of $u(r)$ is from -89.157 at 1.5 Å to -80.11 at 9 Å. Figure 9 shows that the distance dependence of $q_{tet}(r)$ and $u(r)$ for the hydrated α-helix of deca-alanine is very similar to that seen in the β-hairpin of 2GB1.

It is interesting to note that the oscillatory structure of $u(r)$ persists up to 9 Å distance from the peptide. The anticorrelation of $u(r)$ with $q_{tet}(r)$, the similarity in the behavior of the α-helix of deca-alanine and the β-hairpin of 2GB1, and the overall quality of the data suggest that there is a weak layering effect extending at least up to the third neighbor shell. Given the $\langle q_{tet} \rangle$ versus $\langle u \rangle$ data for the different isochores of TIP3P water shown in Figure 5, this variation can be interpreted as a layering effect induced in the medium by the biomolecule. We note that the density as a function of distance from the biomolecule has a sharp peak corresponding to the first hydration layer but is featureless for larger distances.[32,33] It is interesting to speculate whether this long-range effect on the energetics of water molecules surrounding a peptide is somehow related to the existence of very large dynamical hydration shells of biomolecules, with widths of the order of 18 Å, as suggested by recent terahertz spectroscopy experiments.[4]

In order to understand why the distance-dependent tetrahedral order metric and tagged potential energy are anticorrelated, we plot the van der Waals and Coulombic contributions to the TPE for the β-hairpin of 2GB1 in Figure 10. As observed in an earlier study of hydration of collagen helices,[29] $u_{coul}(r)$ and $u_{vdW}(r)$ are anticorrelated with an oscillatory structure, with the dominant $u_{coul}(r)$ contribution determining the behavior of $u(r)$. This implies that $q_{tet}(r)$ must be strongly correlated with $u_{vdW}(r)$ and anticorrelated with $u_{coul}(r)$ for water molecules lying outside the first hydration shell. Within the first hydration shell, especially at low temperatures, this relationship tends to break down possibly because short-range effects, especially those due to interactions with side chains of amino acid residues, become important in determining local structure. At 400 K, the long-range oscillations in $u(r)$ and $q_{tet}(r)$ are not seen.

3.3. Residue-Dependent Variations in Energetics and Mobility of Water Molecules within the Hydration Layer. In this section, we consider the TPEs and residence times of water molecules within the first hydration shell, as a function

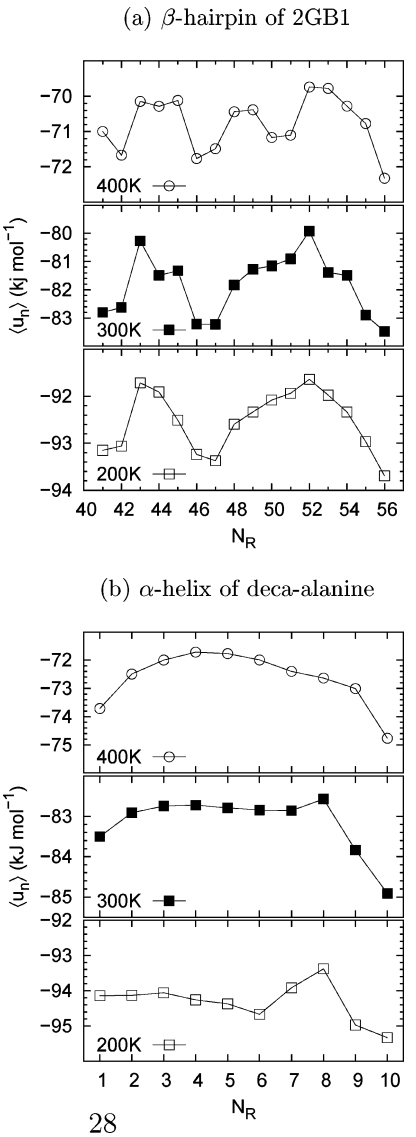

Figure 11. Variation of tagged potential energy along the primary structure for (a) the β-hairpin of 2GB1 and (b) the α-helix of deca-alanine.

of location along the peptide chain. We use $\langle u_n \rangle$ and $\langle \tau_n \rangle$ to denote the TPE energies and residence times of water molecules with O atoms lying within a distance of 5 Å from the C_α atom of residue n. The simplest case to understand is deca-alanine at 400 K, shown in Figure 11a. The C- and N-terminal residues can form hydrogen bonds with water and have a relatively lower TPE. All the others have essentially the same value of $\langle u_{res} \rangle$. As the secondary structure of the helix forms, variations in $\langle u_{res} \rangle$ can be seen, which must reflect the local environment due to the conformational organization of the peptide backbone. At 300 K, there is a distinct lowering in the TPE of water molecules located around residue 9, adjacent to the C-terminal. By 200 K, when the helical structure with three turns is fairly stable, there is a distinct lowering in the $\langle u_6 \rangle$ lying on the central turn of the helix.

We now consider the variations in $\langle u_n \rangle$ for the β-hairpin of the 2GB1 peptide (Figure 11b). In addition to the C-terminal residue, the local minima in $\langle u_n \rangle$ as a function of n occur at $n = 42$ (glutamic acid), $n = 46$ (aspartic acid), and $n = 50$, 51 (lysine, threonine). At this temperature, the secondary structure of the peptide is irrelevant and local electrostatics is clearly the dominant factor affecting $\langle u_n \rangle$. At 300 K, the β-hairpin structure

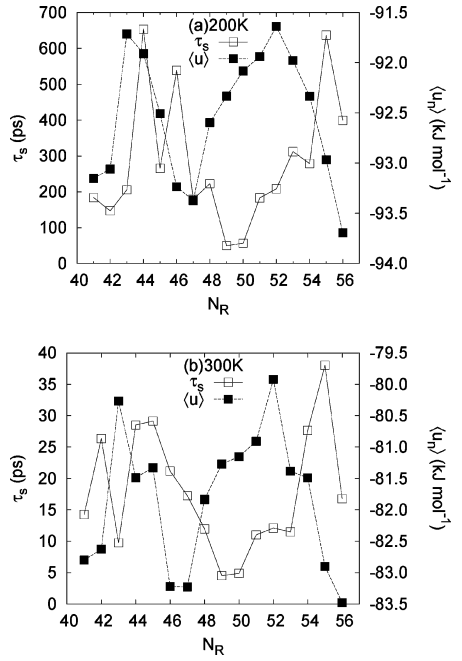

Figure 12. Comparison of tagged potential energy $\langle u \rangle$ and survival correlation times τ_S for the β-hairpin of 2GB1 at (a) 200 K and (b) 300 K.

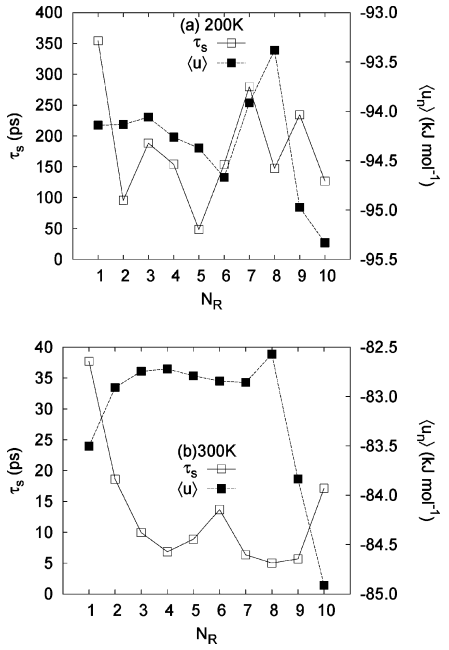

Figure 13. Comparison of tagged potential energy $\langle u \rangle$ and survival correlation times τ_S for the α-helix of deca-alanine at (a) 200 K and (b) 300 K.

is fairly stable and is characterized by the formation of a turn at residues 48 and 49 and the formation of a hydrophobic cluster involving interactions between W43−F52, W43−V54, and Y45−F52.[34] The formation of this secondary structure results in removing the local minimum in $\langle u_n \rangle$ at $n = 50$. The β-hairpin is very stable at 200 K, and the lowest values of TPE are associated with C- and N-terminal amino acids and the two aspartic acid residues adjacent to the β-hairpin turn. Peaks in $\langle u_n \rangle$ occur at tryptophan and phenylalanine, both of which possess large aromatic side chains and are part of the hydrophobic cluster. Comparison with deca-alanine suggests that the chemical identity of residues in addition to the location along the peptide backbone plays a significant role in determining residue-dependent TPEs. In the case of the β-hairpin of 2GB1, the crucial factors determining the residue-dependent TPEs are the presence of charged side chains and the formation of the hydrophobic cluster.

In Figure 12, we compare the residue-dependent variations in the tagged molecule potential energies with the corresponding local residence times for the β-hairpin of the 2GB1 peptide at 200 and 300 K. Figure 13 shows the equivalent plots for the α-helix of deca-alanine. The residence times decrease by about an order of magnitude on going from 300 to 200 K. Interestingly, at a given temperature for a given peptide, the residue-dependent variations in residence times are over a factor of 6, while the variations in TPE are of the order of 3−5%. For the β-hairpin of 2GB1, there is a weak negative correlation between TPE and residence times. Charged residues with low values of local TPE also have relatively large residence times. This supports earlier studies showing that the trends in local residence times are $\tau_{charged} > \tau_{polar} > \tau_{nonpolar}$.[10,65,66] In the case of deca-alanine where all of the residues are identical, the variation in local residence times must be explained by secondary structure formation and coupling of the motions of water molecules in the hydration shell with conformational fluctuations in the protein structure.

The relatively small residue-dependent variation in TPE is, however, likely to be insufficient to completely explain the large variation in residence times. The tagged molecule potential energy is a measure of the local energetics, and it is likely that entropic factors are also significant in determining mobility. Given the recent work on the relationship between structure, entropy, and mobility,[67−69] it would be interesting to further explore structural estimators for the entropy.[3,70]

4. Conclusions

This study examines the extent to which the local energetics of water molecules, as measured by the tagged molecule potential energy (TPE), is modified by the presence of a biomolecular solute, such as a small peptide.

As a benchmark for understanding the perturbation caused by the biomolecular interface, the properties of two common water models, TIP3P and SPC/E, are first considered. We show that TIP3P water has significantly lower local tetrahedral order than SPC/E at the same state point. At 1 g cm^{-3}, the tetrahedral order distribution for bulk TIP3P at 200 K is nearly identical to that of bulk SPC/E at 260 K. This reduction in tetrahedral order in TIP3P is accompanied by a reduction in mean TPE of about 10%. The TIP3P and SPC/E water models show very similar dynamical correlations in the TPE fluctuations on frequency scales greater than 0.1 cm^{-1}, indicating that the short-time dynamics of the two model waters may be very similar, despite well-known differences in equilibrium diffusivities. In addition, the two models show the same linear correlation between mean tetrahedral order and binding energy. The relationship between choice of water models and simulated hydration behavior may thus involve a complex interplay of static and dynamic factors.

The introduction of a peptide in water modifies the local TPE of water molecules as a function of distance from the biomolecular interface. There is an oscillatory variation in the TPE with distance from the peptide for water molecules lying outside a 3 Å radius. These variations are of the order of 2−5% of the bulk TPE value and are anticorrelated with variations in local tetrahedral order in terms of locations of maxima and minima, though the clear linear correlation seen in bulk water is not

observed. The variations in the local order are correlated with those seen in the van der Waals contribution to the TPE, while the Coulombic contribution dominates the tagged molecule potential energy. The oscillatory variations in local order and energetics extend up to at least 10 Å from the peptide surface and suggest a layering effect on the water structure and energetics due to the presence of the peptides. The distance-dependent variations in local order and energetics are essentially the same for the β-hairpin of 2GB1 as well as deca-alanine, suggesting that residue-dependent variations in local properties of the solvent must be confined to the innermost hydration layer.

Within a radius of 3 Å, the perturbation of the solvent structure is very significant with local TPEs that are 10−15% lower than the bulk value. The chemical identities of side-chain residues and the secondary structure play an important role in determining residue-dependent variations in the TPEs. A comparison of the β-hairpin of 2GB1 and deca-alanine shows that the residue-dependent TPEs are sensitive to the presence of charged residues and the formation of a hydrophobic core stabilizing the hairpin structure. The variation in the residue-dependent tagged molecule potential energies is of the order of 3−5%, while the local residence times vary by a factor of approximately 5. Thus, the correlation of the local mobility with the local energetics within the innermost hydration layer is relatively weak with the charged residues associated with low binding energies and large residence times of local water molecules.

The key conclusions and implications of this study for future work may be summarized as follows. The TIP3P and SPC/E model both show qualitatively similar relationships between local energy and tetrahedral order. At a given temperature, the extent of tetrahedral order in bulk TIP3P is significantly lower than that for SPC/E. This implies that, close to ambient conditions, TIP3P will tend to behave as a simple liquid, rather than an anomalous one, which would have significant implications for hydrophobic solvation. In terms of solvation of ions or polar solutes, it is important to note that TIP3P and SPC/E have almost identical dipole moments but different quadrupole moments. This has been shown to be a critical factor in determining the phase diagram of water and may contribute to differences in the structural organization of the solvent around a solute. The tagged potential energies in the innermost hydration layer of a peptide are 10−15% lower than bulk water and show significant residue-dependent variations. Outside of this innermost shell, there is an oscillatory variation in the tagged potential energy which is anticorrelated with the tetrahedral order and can be explained by considering the decomposition of the tagged potential energy into van der Waals and Coulombic contributions. This intermediate range oscillatory behavior is present at 200 and 300 K in the hydration shells of both the 2GB1 β-hairpin and deca-alanine. A similar behavior in the tagged potential energy has been observed earlier in the case of collagen hydration.[29] Since it originates in the negative correlation between binding energy and tetrahedral order of bulk water, it is likely to be present for all standard water models. A final observation from this study is that residue-dependent variations in residence times of water molecules within the first hydration shell vary much more strongly than the tagged potential energies, suggesting that entropic factors and collective motions of the peptides may be important factors in determining local mobility within the hydration layer. In this context, in view of cumulant-type expansions of the chemical potential mentioned in the introductions, it may be interesting to examine fluctuations in the tagged potential energies. An alternative approach would be to consider defining scaling relationships between local measures of diffusivity and entropy, analogous to the excess entropy scaling relationships seen in bulk liquids.[11,71,72]

Acknowledgment. C.C. and M.A. thank the Department of Science and Technology and the Indian Institute of Technology, respectively, for financial support. H.R.K. thanks Jawaharlal Nehru University and Council for Industrial and Scientific Research for financial support.

References and Notes

(1) Bellissent-Funel, M.-C., Ed. *Hydration Processes in Biology*; IOS Press: Amsterdam, The Netherlands, 1999.
(2) Bagchi, B. *Chem. Rev.* **2005**, *105*, 3197.
(3) Li, Z.; Lazaridis, T. *Phys. Chem. Chem. Phys.* **2007**, *9*, 573.
(4) Born, B.; Kim, S. J.; Ebbinghaus, S.; Gruebele, M.; Havenith, M. *Faraday Discuss.* **2009**, *141*, 161.
(5) Qvist, J.; Persson, E.; Mattea, C.; Halle, B. *Faraday Discuss.* **2009**, *141*, 131.
(6) Mishima, O.; Stanley, H. E. *Nature* **1998**, *396*, 329.
(7) Errington, J. R.; Debenedetti, P. G. *Nature* **2001**, *409*, 318.
(8) Debenedetti, P. G. *J. Phys.: Condens. Matter* **2003**, *15*, R1669.
(9) Chandler, D. *Nature* **2005**, *437*, 640.
(10) Merzel, F.; Smith, J. C. *Proc. Natl. Acad. Sci.* **2002**, *99*, 5378.
(11) Sharma, R.; Chakraborty, S. N.; Chakravarty, C. *J. Chem. Phys.* **2006**, *125*, 204501.
(12) Sharma, R.; Agarwal, M.; Chakravarty, C. *Mol. Phys.* **2008**, *106*, 1925.
(13) Vega, C.; Sanz, E.; Abascal, J. L. F.; Noya, E. G. *J. Phys.: Condens. Matter* **2009**, *20*, 153101.
(14) Kumar, P.; Franzese, G.; Stanley, H. E. *J. Phys.: Condens. Matter* **2008**, *20*, 244114.
(15) Paschek, D. *J. Chem. Phys.* **2004**, *20*, 6674.
(16) Lynden-Bell, R. M.; Head-Gordon, T. *Mol. Phys.* **2006**, *104*, 3593.
(17) Buldyrev, S. V.; Kumar, P.; Debenedetti, P. G.; Rossky, P. J.; Stanley, H. E. *Proc. Natl. Acad. Sci.* **2007**, *104*, 20177.
(18) Soper, A. K. *Physica B* **2000**, *276*, 12.
(19) Melchionna, S.; Briganti, G.; Londei, P.; Cammarano, P. *Phys. Rev. Lett.* **2004**, *92*, 158101.
(20) Lee, S. L.; Debenedetti, P. G.; Errington, J. R. *J. Chem. Phys.* **2005**, *122*, 204511.
(21) Mudi, A.; Chakravarty, C. *J. Phys. Chem. B* **2004**, *108*, 19607; **2006**, *110*, 4502.
(22) Mudi, A.; Chakravarty, C.; Ramaswamy, R. *J. Chem. Phys.* **2005**, *122*, 104507; **2006**, *124*, 069902.
(23) Mudi, A.; Ramaswamy, R.; Chakravarty, C. *Chem. Phys. Lett.* **2005**, *376*, 683.
(24) Mudi, A.; Chakravarty, C. *J. Phys. Chem. B* **2006**, *110*, 8422.
(25) Sharma, R.; Chakravarty, C. *J. Phys. Chem. B* **2008**, *112*, 9071; **2009**, *113*, 7965.
(26) Murdock, S. E.; Lynden-Bell, R. M.; Kohanoff, J.; Sexton, G. J. *Phys. Chem. Chem. Phys.* **2002**, *4*, 3016.
(27) Garde, S.; Garcia, A. E.; Pratt, L. R.; Hummer, G. *Biophys. Chem.* **1999**, *78*, 21.
(28) Pratt, L. R.; Hummer, G.; Garcia, A. E. *Biophys. Chem.* **1994**, *51*, 147.
(29) Handgraaf, J.-W.; Zerbetto, F. *Proteins* **2006**, *64*, 711.
(30) Bandyopadhyay, S.; Chakraborty, S.; Balasubramanian, S.; Pal, S.; Bagchi, B. *J. Phys. Chem. B* **2004**, *108*, 12608.
(31) Bandyopadhyay, S.; Chakraborty, S.; Balasubramanian, S.; Bagchi, B. *J. Am. Chem. Soc.* **2005**, *127*, 4071.
(32) Bandyopadhyay, S.; Chakraborty, S.; Bagchi, B. *J. Am. Chem. Soc.* **2005**, *127*, 16660.
(33) Bandyopadhyay, S.; Chakraborty, S.; Bagchi, B. *J. Phys. Chem. B* **2006**, *110*, 20629.
(34) Munoz, V.; Thompson, P. A.; Hofrichter, J.; Eaton, W. A. *Nature* **1997**, *390*, 196.
(35) Dinner, A. R.; Lazaridis, T.; Karplus, M. *Proc. Natl. Acad. Sci.* **1999**, *96*, 9068.
(36) Bolhuis, P. G. *Proc. Natl. Acad. Sci.* **2003**, *100*, 12129.
(37) Zhou, R.; Berne, B. J.; Germain, R. *Proc. Natl. Acad. Sci.* **2001**, *98*, 14931.
(38) Garcia, A. E.; Sanbonmatsu, K. Y. *Proteins* **2001**, *42*, 345.
(39) Tsai, J.; Levitt, M. *Biophys. Chem.* **2002**, *101*, 187.
(40) Roccatano, D.; Amadei, A.; Nola, A. D.; Berendsen, H. J. *Protein Sci.* **1999**, *8*, 2130.
(41) Jang, S.; Kim, E.; Pak, Y. *Proteins* **2007**, *66*, 53.
(42) Zhang, L.; Hermans, J. *J. Am. Chem. Soc.* **1994**, *116*, 11915.
(43) Garcia, A. E.; Hummer, G.; Soumpasis, D. M. *Proteins* **1997**, *27*, 271.

(44) Park, S.; Khalili-Araghi, F.; Tajkhorshid, E.; Schulten, K. *J. Chem. Phys.* **2003**, *119*, 3559.
(45) Mezei, M.; Fleming, P. J.; Srinivasan, R.; Rose, G. D. *Proteins* **2004**, *55*, 502.
(46) MacKerell, A. D.; et al. *J. Phys. Chem. B* **1998**, *102*, 3586.
(47) Nutt, D. R.; Smith, J. C. *J. Chem. Theory Comput.* **2007**, *3*, 1550.
(48) Leach, A. R. *Molecular Modelling*; Addison Wesley Longman: China, 1998.
(49) Vega, C.; Abascal, J. L. F. *J. Chem. Phys.* **2005**, *123*, 144504.
(50) Berendsen, H. J. C.; Grigera, J. R.; Straatsma, T. P. *J. Phys. Chem.* **1987**, *91*, 6269.
(51) Jorgensen, W.; et al. *J. Chem. Phys.* **1983**, *79*, 926.
(52) Humphrey, W.; Dalke, A.; Schulten, K. *J. Mol. Graphics* **1996**, *14*, 33.
(53) Smith, W.; Yong, C. W.; Rodger, P. M. *Mol. Simul.* **2002**, *28*, 385. The DLPOLY website is http://www.cse.clrc.ac.uk/msi/software/DL_POLY.
(54) Phillips, J. C.; Braun, R.; Wang, W.; Gumbart, J.; Tajkhorshid, E.; Villa, E.; Chipot, C.; Skeel, R. D.; Kal Schulten, K. *J. Comput. Chem.* **2005**, *26*, 1781.
(55) Chau, P.-L.; Hardwick, A. J. *Mol. Phys.* **1998**, *93*, 511.
(56) The tagged potential energy was computed using the *pairInteraction* keyword of NAMD, once the simluation itself was over.
(57) Lee, S. H.; Rasaiah, J. C. *J. Phys. Chem.* **1996**, *100*, 1420.
(58) Laage, D.; Hynes, J. T. *J. Phys. Chem. B* **2008**, *112*, 7697.
(59) Koneshan, S.; Rasaiah, J. C.; Lynden-Bell, R. M.; Lee, S. H. *J. Phys. Chem. B* **1998**, *102*, 4193.
(60) Jhon, Y. I.; No, K. T.; Jhon, M. S. *Fluid Phase Equilib.* **2006**, *244*, 160.
(61) Jhon, Y. I.; No, K. T.; Jhon, M. S. *J. Phys. Chem. B* **2007**, *111*, 9897.
(62) Agarwal, M.; Alam, M. P.; Chakravarty, C. Manuscript in preparation.
(63) Sharma, R.; Mudi, A.; Chakravarty, C. *J. Chem. Phys.* **2006**, *125*, 044705; **2009**, *130*, 199903.
(64) There are small differences in the values of α and the frequency of crossover to white noise for SPC/E water as published here and in refs 22 and 63. A computational error in the earlier work was recently corrected, and the associated error is discussed in ref 25.
(65) Garcia, A. E.; Stiller, L. *J. Comput. Chem.* **1993**, *14*, 1396.
(66) Rocchi, C.; Bizzarri, A. R.; Cannistraro, S. *Chem. Phys.* **1997**, *214*, 261.
(67) Errington, J. R.; Truskett, T. M.; Mittal, J. *J. Chem. Phys.* **2006**, *125*, 244502.
(68) Agarwal, M.; Chakravarty, C. *J. Phys. Chem. B* **2007**, *111*, 13294.
(69) Agarwal, M.; Sharma, R.; Chakravarty, C. *J. Chem. Phys.* **2007**, *127*, 164502.
(70) Kuffel, A.; Zielkiewicz, J. *J. Phys. Chem. B* **2008**, *112*, 15503.
(71) Agarwal, M.; Chakravarty, C. *Phys. Rev. E* **2009**, *79*, 030202.
(72) Mittal, J.; Truskett, T. M.; Errington, J. R.; Hummer, G. *Phys. Rev. Lett.* **2008**, *100*, 145901.

JP909090U